

# UC Davis

## UC Davis Previously Published Works

### Title

Alterations in the proteome of the respiratory tract in response to single and multiple exposures to naphthalene

### Permalink

<https://escholarship.org/uc/item/1d57d89c>

### Journal

Proteomics, 15(15)

### ISSN

1615-9853

### Authors

Kültz, Dietmar  
Li, Johnathon  
Sacchi, Romina  
et al.

### Publication Date

2015-08-01

### DOI

10.1002/pmic.201400445

Peer reviewed



Published in final edited form as:

*Proteomics*. 2015 August ; 15(15): 2655–2668. doi:10.1002/pmic.201400445.

## Alterations in the proteome of the respiratory tract in response to single and multiple exposures to naphthalene

Dietmar Kültz<sup>1</sup>, Jonathan Li<sup>1</sup>, Romina Sacchi<sup>1</sup>, Dexter Morin<sup>2</sup>, Alan Buckpitt<sup>2</sup>, and Laura Van Winkle<sup>3</sup>

<sup>1</sup>Department of Animal Science, College of Agricultural and Environmental Sciences, University of California, Davis, CA 95616

<sup>2</sup>Department of Molecular Biosciences, School of Veterinary Medicine, University of California, Davis, CA 95616

<sup>3</sup>Department of Anatomy, Physiology and Cell Biology, School of Veterinary Medicine, University of California, Davis, CA 95616

### Abstract

Protein adduction is considered to be critical to the loss of cellular homeostasis associated with environmental chemicals undergoing metabolic activation. Despite considerable effort, our understanding of the key proteins mediating the pathologic consequences from protein modification by electrophiles is incomplete. This work focused on naphthalene-induced acute injury of respiratory epithelial cells and tolerance which arises after multiple toxicant doses to define the initial cellular proteomic response and later protective actions related to tolerance. Airways and nasal olfactory epithelium from mice exposed to 15 ppm NA either for 4 hrs (acute) or for 4 hrs/day  $\times$  7 days (tolerant) were used for label free protein quantitation by LC/MS/MS. Cyp2f2 and secretoglobin 1A1 are decreased dramatically in airways of mice exposed for 4 hrs, a finding consistent with the fact that P450's are localized primarily in Clara cells. A number of heat shock proteins and protein disulfide isomerases, which had previously been identified as adduct targets for reactive metabolites from several lung toxicants, were upregulated in airways but not olfactory epithelium of tolerant mice. Protein targets that are upregulated in tolerance may be key players in the pathophysiology associated with reactive metabolite protein adduction.

### Keywords

Clara cells; metabolic activation; naphthalene; protein adduct

### Introduction

The introduction and wide spread application of methods for measuring the transcriptome in the 1990's was hailed in the scientific community as a key step in understanding the differences between diseased and normal cells. Transcriptomic approaches also offered a

strategy for monitoring early stage disease and, along with it, the identification of potential therapeutic targets[1]. At this same time, substantial effort was directed toward understanding patterns of gene expression associated with the toxicity of chemicals with the expectation that a fingerprint of increased or decreased expression of certain genes could be used as markers for potential cellular injury and that these signatures would serve as a predictive screen to eliminate problem candidate compounds from the drug development pipeline [2]. While these broadscale transcriptomic approaches have provided important new information regarding disease targets and have generated useful methods for classifying the safety profile of some chemicals [3], they have not proven to be as predictive as once hoped. There are likely several reasons for this including the poor correlations between the transcriptome and the proteome (reviewed in [4]) and the fact that posttranslational modifications often modulate the functions of cellular proteins. Monitoring changes in the proteome, while technically more challenging, is likely to provide a better assessment of cellular changes that are more closely tied to phenotypic alterations in the cell. Understanding the proteomic response to chemical toxicants can provide important insights regarding the fundamental mechanisms by which these agents disrupt the cellular machinery and afford biomarker targets for further development as early disease markers.

Over the past several years, a number of laboratories including ours have focused on identifying proteins that are adducted by reactive metabolites generated via cytochrome P450 dependent activation of chemicals that produce cytotoxic injury in the respiratory tract. These chemicals include butylated hydroxytoluene [5, 6], 1-nitronaphthalene [7, 8] and naphthalene [9, 10]. The overall goal has been to probe fundamental mechanisms by which these agents disrupt cellular homeostasis. While many of the protein targets identified with reactive metabolites generated in the lung are the same as those reported in the liver with hepatotoxic agents [11], these studies serve only to provide a list of possible suspects associated with the disruption of cellular homeostasis. Although these studies have shown: 1) that adduct formation is not limited only to the most abundant proteins [7, 12], 2) that the extent of modification is generally modest [13, 14] and 3) that there are multiple amino acid targets for most of the reactive metabolites [15, 16], they provide very little information on which protein or, more likely, group of proteins are intimately associated with the events that lead to cellular necrosis [17]. One strategy to begin to discriminate those adductions which occur on proteins which are critical to cell survival compared to bystander proteins is to understand alterations in the proteome of target cells during initial stages of injury and after multiple exposures where target cells become resistant to injury.

The work described here was done using naphthalene, a model, highly selective toxicant to the respiratory tract of mice where the cellular alterations in both the airway and nasal epithelial cells have been well characterized following exposure by the inhalation or parenteral routes of exposure. Acute 4 hr inhalation exposures to 15 ppm naphthalene resulted in swelling and vacuolization of Clara cells in the airway epithelium which were visible immediately at the end of the exposure and progressed to necrosis and exfoliation of airway epithelial Clara cells 24 hrs after the start of the exposure [18]. In comparison, the nasal olfactory epithelium appeared normal 0–4 hrs following the end of a 15 ppm exposure but at 20 hrs after the end of the exposure, olfactory epithelial cells were nearly completely absent from the nasal ethmoid tissue. Multiple doses of naphthalene, administered either

intraperitoneally or by inhalation daily for 7 days result in tolerance to large, challenge doses [19, 20]. The toxicity of naphthalene is dependent on the cytochrome P450-dependent metabolic activation of the parent substrate to electrophilic metabolites and the formation and disposition of these metabolites correlates with the extent of injury in the lung (see [21] for review).

In the current study, we applied highly sensitive LC/MS/MS approaches to samples from target areas of the respiratory tract to probe changes in expression profiles of proteins in the olfactory and intrapulmonary airway epithelium in response to both single and multiple naphthalene exposures. The data presented here focus primarily on those proteins which had previously been shown to be adducted by reactive metabolites of naphthalene although a complete database of the alterations in protein abundance observed in response to naphthalene is available online (<http://www.ebi.ac.uk/pride/>). We reasoned that adducted, critical proteins would be at higher levels in naphthalene tolerant animals and that those that were either at lower levels or remained the same are acting as bystander proteins.

## Materials and Methods

### Animals

All animal work was conducted under protocols approved by the University of California – Davis Animal Use and Care Committee (IACUC number 17103, AALAC number A3433-01). Male Swiss-Webster mice (25–30g) were purchased from Harlan (Livermore, CA) and allowed free access to food and water. Animals were housed in HEPA-filtered isolators in an AAALAC accredited facility for one week before use. All treated and control groups in this study contained 6 mice.

### Inhalation exposures

Naphthalene was generated by passing filtered, compressed air through a column containing crystalline naphthalene as described in detail previously [22]. This was mixed with compressed air in a mixing chamber; vapor concentrations were monitored continuously by passing the samples through a UV flow cell using a wavelength of 211 nm. Mice (3 per cage) were exposed in all-glass metabolism chambers to 15 ppm naphthalene for 4 hrs; controls were exposed to filtered air. All exposures were concluded before 1 pm to avoid differences associated with the diurnal variations in glutathione levels. Two separate experiments with 6 control and 6 exposed mice were conducted with the short term exposures. In one case, animals were euthanized within 90 min of exposure to determine the effects of initial chemical insult where airway epithelium begins to show morphological changes but where the airway itself is not exfoliated. A second group of 6 control and 6 treated animals was exposed for 4 hrs but animals were euthanized 24 hrs following the end of the exposure. This is a time point where moderately severe injury to the epithelium has occurred and many cells have exfoliated from the airways. A further group of 6 control and 6 treated mice were exposed to naphthalene 4 hrs per day for 7 days to induce tolerance [20].

## Preparation of tissues for proteomic analysis

Mice were euthanized either 90 min or 24 hrs following the conclusion of the short term, 4 hr exposure with an overdose of pentobarbital. The trachea was cannulated and lungs filled with low melting agarose for airway dissection as described previously [23]. The tolerant animals were euthanized 24 hrs after the seventh day of exposure to naphthalene. Airways were placed directly on dry ice for subsequent analysis. The head was removed, skinned, the lower jaw was excised and the skull divided along the longitudinal suture line. Olfactory epithelium was removed by dissection and placed immediately on dry ice.

### Protein extraction and preparation of samples for LC/MS/MS analysis—

Procedures for the extraction of proteins from the sample and preparation for analysis have been described in detail in another manuscript [24]. Briefly, frozen tissues were pulverized at liquid nitrogen temperatures using a ceramic mortar and pestle. Proteins were washed at 4°C with 10% TCA/0.2% DTT (90:10) overnight. Proteins were pelleted by centrifugation, washed twice with ice cold acetone containing 0.2% DTT and samples were dissolved in 7 M urea, 2 M thiourea/0.2% DTT. Aliquots of the dissolved sample were assayed for protein using the Thermo-Pierce 660 nm kit with BSA as the standard. Samples were diluted to 1.5 µg/µl, DTT was added, samples were incubated at 55°C and sulfhydryls were derivatized by the addition of iodoacetamide to a final concentration of 16 mM. Samples were digested with immobilized trypsin (Princeton Separations, Freehold Township, NJ) for 16 hrs at 35°C, were concentrated on a vacuum centrifuge and redissolved in 0.1% formic acid.

**LC/MS/MS analysis—**A complete description of the separation, and MS/MS analysis of tryptic peptides for label free quantitative comparison of peptide/protein abundance of samples extracted from tissue has been provided in a separate paper [24]; an abbreviated description is provided here. Each sample was trapped for 3 min on a Waters Symmetry trap column (0.18 × 20 mm, 5µ) followed by elution to a BEH C<sub>18</sub> column (250 mm × 75 µm) with 0.1% formic acid and acetonitrile as the eluting solvents. Tryptic peptides were eluted with a 70 min linear gradient from 3 to 35% ACN. A nanoAcquity solvent manager was used to deliver solvent at a flow rate of 300 nL/min. Column eluent was delivered to a nano-ESI source and analysis performed on a Bruker Daltonics microQTOF II mass spectrometer. Data were processed using Hystar 3.2 software (Bruker) and peak lists were generated with Mascot Daemon and Distiller (Matrix Sciences). Mascot 2.2 (Matrix Science) and Phenix 2.6 (Geneva Bioinformatics) were used for protein identification and search results were combined in Proteinscape 3.1 (Bruker Daltonics). The complete mouse proteome containing 42895 protein sequences was downloaded from UniProtKB on August 8, 2013 and for each protein sequence a randomly scrambled decoy sequence was generated using PEAKS 6 (Bioinformatics Solutions). This decoy database containing 85790 total entries, was used to search peak lists and false discovery rate was determined from the number of decoy sequences present in the search results. Using this decoy database, a false discovery rate (FDR) limit of 3% was applied to all protein IDs. Spectra were analyzed using the following parameters: maximum of 2 missed cleavages, Cys carbidomethylation, variable modifications including methionine oxidation, proline hydroxylation and N-terminal protein acetylation, a 20 ppm precursor ion tolerance and a fragment ion mass tolerance of 0.1 Da. Protein scores for the MS/MS spectra all exceeded a 5% threshold for the possibility of

incorrect identification. All data for this project are posted on the PRIDE web site (<http://www.ebi.ac.uk/pride/>) which allows the user to review data on mass error distributions, missed cleavage frequencies and the number of identified peptides. The PRIDE project accession number is PRD000846, PRIDE experiment accession numbers are 30584 and 30585.

Quantitative profiling was accomplished with the aid of ProfileAnalysis 2.0 and Proteinscape 3.1 from Bruker Daltonics. Alignment and integration of the chromatographic peaks relied on the ProfileAnalysis software wherein precursor ions with an intensity exceeding  $10^3$  counts for 10 consecutive MS scans were scored as positive. Positive matches were scored only if on multiple runs, retention time was within 1 min and the peptide mass deviated less than 20 ppm. Spectral counting was performed after importing the data into Scaffold 4.0 (Proteome Systems). A select group of proteins showing alterations in abundance in response to naphthalene either following a single dose or multiple (tolerance-inducing) doses were selected for further analysis by accurate mass and time tag (AMT) analysis as previously described [24].

**Detection of glycosylated peptides**—Proteinscape 3.1 (Bruker Daltonics) was used to detect and annotate glycans and the corresponding glycoproteins. MS/MS spectra were first classified as glycopeptides using the following parameters: min  $m/z = 700$ ,  $m/z$  signals = oxonium ions CID positive, mass tolerance = 0.02 Da, min. intensity coverage = 10%, min. # of consecutive  $m/z$  distances required = 2, distance tolerance = 0.02 Da, min. peptide mass = 1000 Da. Glycans were then detected on spectra classified as glycopeptides using the GlycomeDB database [25] as the reference and score, intensity coverage, and fragmentation coverage thresholds of 10%. Finally, glycan structures were assigned to glycoproteins by combining them with Mascot and Phenyx protein search results in Proteinscape 3.1.

## Results and Discussion

### Label Free Quantitative Analysis of Airway and Nasal Olfactory Proteins

These studies utilized dissected airways from 6 treated animals compared to 6 controls. Technical replicates were performed with animals exposed to naphthalene acutely to determine data consistency. A range of 2–84 peptides with an average of 12 peptides per identified protein that fit the criteria (retention time within 1 min, a 20 ppm precursor ion tolerance and at least 1000 counts on 10 consecutive scans) yielded data with an average FDR less than 3%. As is common with proteomics data, not every protein was detected during each analysis.

### Overall changes in the abundance of proteins in airways and nasal olfactory epithelium in response to naphthalene exposure

A number of airway and nasal olfactory epithelial proteins were up and down regulated following a single acute exposure to naphthalene and after 7 exposures that lead to tolerance (Figure 1). More proteins in the nasal epithelium respond to naphthalene exposure than airway proteins and this is consistent with the finding that nasal epithelium removes 50–60% of the inhaled naphthalene [26]. Forty to 50% of the proteins that were increased in nasal

olfactory epithelium following an acute exposure were also increased after 7 daily exposures. Nearly  $\frac{3}{4}$  of the proteins down regulated by the acute exposure were also decreased following multiple exposures. Not only were fewer proteins modulated by both acute and 7 day naphthalene exposures in the airway than in the nasal olfactory epithelium but there was far less overlap of the same protein being either increased or decreased after both acute and 7 day exposures. A complete list of the proteins where the levels are altered is included in the pride data base.

### Response of proteins identified as adduct targets to naphthalene exposure

Previous studies from our laboratory and others have identified more than 100 non redundant proteins that are adducted by reactive metabolites generated from lung toxicants including butylated hydroxytoluene, 1-nitronaphthalene, monocrotalin pyrrole, 1,4-naphthoquinone, 1,4-benzoquinone and naphthalene ([http://tpdb.medchem.ku.edu:8080/protein\\_database/search.jsp](http://tpdb.medchem.ku.edu:8080/protein_database/search.jsp)). These are all chemicals with established cytotoxic effects in the lung either when tested *in vivo* or, in some cases, in cell preparations derived from the lung. Of the more than 100 different proteins which have been identified as adduct targets, nearly 20% are either up or down regulated in response to naphthalene treatment (Table 1). Of particular interest are those proteins associated with the unfolded protein response as well as antioxidant proteins. These included several of the heat shock proteins, protein disulfide isomerase A3 and calreticulin which were all at increased levels in the airways of naphthalene-tolerant animals in comparison to the air controls. Heat shock proteins are adduct targets for a number of bioactivated chemicals [27] including several that are lung selective (Table 1). Furthermore, recent studies have shown that several of the heat shock proteins are adducted by 4-hydroxynonenal, a reactive breakdown product of lipid peroxidation [28], and that siRNA knock down of the transcription factor, HSF1, whose translocation to the nucleus is controlled by several of the HSP's markedly enhances the loss in cell viability associated with HNE exposure [29]. Likewise, brief treatment of A549 lung cells with heat altered the distribution of HSP 90 to intermediate filaments and this correlated well with protection from another Michael adducting carbonyl, acrolein [30]. Finally, HSP 70i knockout mice are considerably more susceptible to the hepatotoxic effects of acetaminophen, a bioactivated liver toxicant [31]. Taken together all of these findings show that 1) HSP's are adducted by a wide variety of electrophiles 2) that alterations which either decrease (siRNA, knockout) or increase HSP's (heat shock pretreatment, naphthalene tolerance) serve to alter the susceptibility of tissues/cells to toxicity associated with the presence of electrophilic intermediates. All of these studies are consistent with a detailed, recently published bioinformatics approach which considers the effects on protein interacting partners and which suggests that several of the strongest links to toxicity arise from the interactions of reactive metabolites with heat shock proteins [32].

### Naphthalene-reactive proteins are glycosylated

Most proteins adducted by reactive naphthalene metabolites are N- or O-glycosylated in lung airway epithelium (LAE) (Fig 2, Table 2). This is not the case in nasal olfactory epithelium (NOE), superoxide dismutase being the exception. Overall protein and peptide coverage is roughly comparable between the tissues with 15,889 peptides mapped to 737 proteins in LAE and 10,262 peptides mapped to 919 proteins in NOE (PRIDE Project

accession PRD000846). Nevertheless, sequence coverage (mean  $\pm$  SEM for the set of proteins considered here) differs significantly between LAE ( $61.6 \pm 3.3\%$ ) and NOE ( $47.2 \pm 3.9\%$ , t-test  $p < 0.005$ , Supplemental Table 1). It is possible, but seems unlikely, that this relatively small difference in sequence coverage represents the main reason for the tissue-specific difference in protein glycosylation. That posttranslational protein glycosylation is a quantitatively significant modification is well established as are the roles for these modifications in protein folding, transport of modified proteins to the Golgi and other intracellular organelles. Glycosylated proteins appear to be excellent targets as biomarkers associated with lung cancer and recent global assessments of the glycoproteome suggest a functional role for these modifications in lung adenocarcinomas [33, 34]. There is emerging evidence that RAGE (receptor for advanced glycation end products), a member of the immunoglobulin superfamily of cell surface receptors in the lung, and its binding ligands (advanced glycation end products) are important in the downstream signaling associated with a number of inflammatory lung diseases including asthma and COPD (for review see [35, 36]).

### **Increases and decreases in levels of non adducted proteins in response to naphthalene exposure**

The abundance of several proteins changed in response to naphthalene treatment (Figure 1) and several of these have been shown in other studies to be altered by exposure to various chemical insults or to be markers of human lung disease. Markedly increased levels of Chitinase 3 like protein 3 (also known as Ym1) in nasal olfactory epithelium were measured by accurate mass and time tags following an acute exposure to naphthalene with animals killed 24 hrs after exposure (Figure 1). Chitinase proteins are a family of glycosyl hydrolase proteins that are widely expressed in tissues of both pro- and eukaryotes. Ym1 and Ym2 (chitinase 3 like protein 1) are murine proteins which are increased dramatically in the respiratory tract in response to a number of external challenges including inflammation, and oxidant-induced injury [37–39] and appear to be important in modulating the inflammatory and repair responses of the lung in animal models [40]. Levels of the human orthologous protein (YKL-40) correlate well with the incidence and severity of asthma [41]. Galectin 3 was increased in nasal epithelium 24 hrs following acute naphthalene exposure and in nasal and lung airway epithelium following 7 daily exposures, a finding consistent with other studies showing increases in galectin-3 in response to pulmonary toxicants [42]. Studies in Gal-3 KO mice suggest that this galactoside binding lectin plays a role in the remodeling associated with allergic airway disease [43].

Although the studies reported in this manuscript were focused primarily on proteins that have been shown in previous studies to be targeted by reactive metabolites, the expression of a number of other proteins was altered dramatically by naphthalene exposure. These have not been connected previously to changes in protein expression in response to chemical insult but are discussed here to provide a baseline for further understanding of the functional role of these proteins in response to cellular perturbations. Clusterin/apolipoprotein J is a glycoprotein expressed in many tissues and the protein appears to play a role as a molecular chaperone during early stages of oxidative stress but then seems to protect tumor cells and enhance metastases in more advanced stages of tumorigenesis [44]. The expression of



mRNA for clusterin is markedly down regulated in sinonasal adenomas, a rare tumor primarily associated with exposure to wood dust [45]. In contrast, both single and multi day exposures to cytotoxic concentrations of naphthalene increased clusterin expression 3–4 fold in nasal epithelium (Fig 1), a result that is likely related to alterations of cellular redox balance. Similarly, annexin A1 was upregulated 2 fold in nasal olfactory epithelium following both single and multiple inhalation exposures to naphthalene. Substantial experimental evidence supports a role of annexin A1 as an anti-inflammatory protein [46]. Annexin-1 null mice are more sensitive than wild type controls to methacholine challenge in ova-sensitized and challenged animals [47]. Moreover, annexin 1 is present in much higher levels in BAL fluid obtained from individuals diagnosed with COPD and/or lung cancer than controls [48] and in smokers compared to non smokers. While the exact functional significance of increased levels of annexin A-1 in naphthalene-challenged mice is not clear, it appears that this protein is upregulated in several lung diseases and may serve in an overall protective capacity.

Two proteins were markedly decreased following acute exposure to naphthalene: Cyp 2f2 and secretoglobin (1A1) (uterglobin, Clara cell secretory protein). Both of these proteins are highly localized in Clara cells [49, 50] and transcript for both are markedly downregulated following naphthalene treatment [51]. Likewise, immunohistochemical studies demonstrated a marked decrease in Cyp 2f2 signal in airway epithelium of naphthalene-tolerant mice [52], a finding consistent with a 4 fold decrease in protein levels measured in the current work. In naphthalene-tolerant animals (15 ppm 4 hrs × 7 days), Cyp2f2 remained at control levels in lung airway epithelium, a finding consistent with data showing no change in the rates of naphthalene metabolism in dissected airways of tolerant mice [53].

Glutathione peroxidase 6 is decreased in the olfactory regions of the nose after both acute (to less than 25% of untreated controls) and 7 day exposures (to approximately 50% of control). The glutathione peroxidases are considered important for the control of cellular H<sub>2</sub>O<sub>2</sub> levels and it is becoming increasingly evident that cellular redox balance is intimately involved in various cellular signaling processes [54, 55]. However, there is little available information on the catalytic function of this protein, the role of GPx6 in maintaining cellular homeostasis or even the tissue distribution although it has been identified in Bowman's gland [56]. Similarly, calretinin was expressed at less than 50% of the control level in nasal olfactory epithelium for animals exposed once as well as those exposed for 7 days. Calretinin is a calcium binding protein that is thought to have a role in odor discrimination. It is upregulated in mice pulse exposed to the odorant, octanal in mice [57].

In summary, these studies present a LC/MS/MS workflow which allows label free quantitation of several hundred proteins in well-defined compartments of the respiratory tract in response to a highly tissue selective, metabolically activated, cytotoxic agent, naphthalene. Earlier studies have identified more than 70 unique proteins which are posttranslationally modified by electrophiles generated from naphthalene but experimental approaches for determining which protein or group of proteins might be structurally or functionally impaired by these modifications and thus lead to cell death are lacking. A possible approach, presented here, was to determine which proteins posttranslationally modified by naphthalene electrophiles are upregulated in naphthalene tolerant mice. Several

of the heat shock proteins are increased 1.5 to 2 fold and this experimental finding is consistent with recent informatic analysis of the protein target data base for reactive chemicals which also suggests strong direct links for these proteins with cytotoxicity [58]. In addition, these studies showed dramatic decreases in the abundance of several proteins in nasal and airway epithelium. These may be excellent targets for biomarker development for lung lavage or nasal wash that could be useful across species and with other lung toxicants.

## Supplementary Material

Refer to Web version on PubMed Central for supplementary material.

## Acknowledgments

This work has been supported by a grant of the Superfund Basic Science Research Program, NIEHS P42 ES 04699 to DK and AB.

## abbreviations

<b>NA</b>	naphthalene
<b>NN</b>	nitronaphthalene
<b>BHT</b>	butylated hydroxytoluene

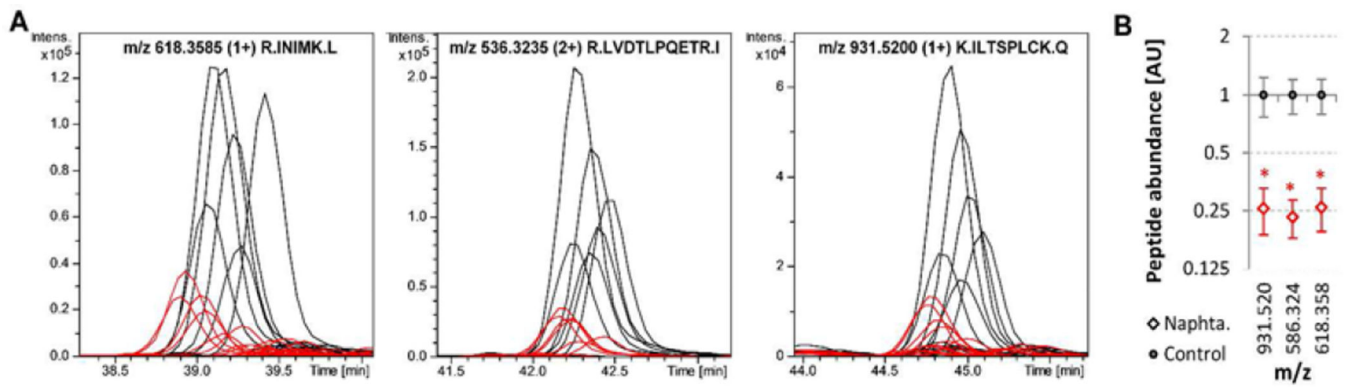
## References

1. Debouck C, Goodfellow PN. DNA microarrays in drug discovery and development. *Nat. Genet.* 1999; 21:48–50. [PubMed: 9915501]
2. Waring JF, Jolly RA, Ciurlionis R, Lum PY, et al. Clustering of hepatotoxins based on mechanism of toxicity using gene expression profiles. *Toxicol. Appl. Pharmacol.* 2001; 175:28–42. [PubMed: 11509024]
3. Thomas RS, Bao WJ, Chu TM, Bessarabova M, et al. Use of short-term transcriptional profiles to assess the long-term cancer-related safety of environmental and industrial chemicals. *Tox Sci.* 2009; 112:311–321.
4. de Sousa Abreu R, Penalva LO, Marcotte EM, Vogel C. Global signatures of protein and mRNA expression levels. *Mol Biosyst.* 2009; 5:1512–1526. [PubMed: 20023718]
5. Meier BW, Gomez JD, Kirichenko OV, Thompson JA. Mechanistic basis for inflammation and tumor promotion in lungs of 2,6-di-tert-butyl-4-methylphenol-treated mice: electrophilic metabolites alkylate and inactivate antioxidant enzymes. *Chem Res Toxicol.* 2007; 20:199–207. [PubMed: 17305404]
6. Meier BW, Gomez JD, Zhou A, Thompson JA. Immunochemical and proteomic analysis of covalent adducts formed by quinone methide tumor promoters in mouse lung epithelial cell lines. *Chem Res Toxicol.* 2005; 18:1575–1585. [PubMed: 16533022]
7. Wheelock AM, Boland BC, Isbell M, Morin D, et al. In vivo effects of ozone exposure on protein adduct formation by 1-nitronaphthalene in rat lung. *Am J Respir Cell Mol Biol.* 2005; 33:130–137. [PubMed: 15845863]
8. Lin CY, Boland BC, Lee YJ, Salemi MR, et al. Identification of proteins adducted by reactive metabolites of naphthalene and 1-nitronaphthalene in dissected airways of rhesus macaques. *Proteomics.* 2006; 6:972–982. [PubMed: 16453347]
9. Lin CY, Isbell MA, Morin D, Boland BC, et al. Characterization of a structurally intact in situ lung model and comparison of naphthalene protein adducts generated in this model vs lung microsomes. *Chem Res Toxicol.* 2005; 18:802–813. [PubMed: 15892573]

10. DeStefano-Shields C, Morin D, Buckpitt A. Formation of covalently bound protein adducts from the cytotoxicant naphthalene in nasal epithelium: species comparisons. *Environ Health Perspect*. 2010; 118:647–652. [PubMed: 20435546]
11. Fang J, Koen Y, Hanzlik R. Bioinformatic analysis of xenobiotic reactive metabolite target proteins and their interacting partners. *BMC Chem. Biol*. 2009; 9
12. Lin CY, Boland BC, Lee YJ, Salemi MR, et al. Identification of proteins adducted by reactive metabolites of naphthalene and 1-nitronaphthalene in dissected airways of rhesus macaques. *Proteomics*. 2006; 6:972–982. [PubMed: 16453347]
13. Ikehata K, Duzhak TG, Galeva NA, Ji T, et al. Protein targets of reactive metabolites of thiobenzamide in rat liver in vivo. *Chem Res Toxicol*. 2008;1432–1442. [PubMed: 18547066]
14. Stamper BD, Mohar I, Kavanagh TJ, Nelson SD. Proteomic Analysis of Acetaminophen-Induced Changes in Mitochondrial Protein Expression Using Spectral Counting. *Chem Res Toxicol*. 2011
15. Pham NT, Jewell WT, Morin D, Buckpitt AR. Analysis of naphthalene adduct binding sites in model proteins by tandem mass spectrometry. *Chem Biol Interact*. 2012; 199:120–128. [PubMed: 22659010]
16. Pham NT, Jewell WT, Morin D, Jones AD, Buckpitt AR. Characterization of model peptide adducts with reactive metabolites of naphthalene by mass spectrometry. *PloS one*. 2012; 7:e42053. [PubMed: 22870282]
17. Monks TJ, Lau SS. Reactive intermediates: molecular and MS-based approaches to assess the functional significance of chemical-protein adducts. *Toxicol Pathol*. 2013; 41:315–321. [PubMed: 23222993]
18. Phimister AJ, Lee MG, Morin D, Buckpitt AR, Plopper CG. Glutathione depletion is a major determinant of inhaled naphthalene respiratory toxicity and naphthalene metabolism in mice. *Toxicol Sci*. 2004; 82:268–278. [PubMed: 15319489]
19. O'Brien KA, Suverkropp C, Kanekal S, Plopper CG, Buckpitt AR. Tolerance to multiple doses of the pulmonary toxicant, naphthalene. *Toxicol Appl Pharmacol*. 1989; 99:487–500. [PubMed: 2749735]
20. West JA, Van Winkle LS, Morin D, Fleschner CA, et al. Repeated inhalation exposures to the bioactivated cytotoxicant naphthalene (NA) produce airway-specific Clara cell tolerance in mice. *Toxicol Sci*. 2003; 75:161–168. [PubMed: 12805647]
21. Buckpitt A, Boland B, Isbell M, Morin D, et al. Naphthalene-induced respiratory tract toxicity: metabolic mechanisms of toxicity. *Drug Metab Rev*. 2002; 34:791–820. [PubMed: 12487150]
22. West J, Pakenham G, Morin D, Fleschner C, et al. Inhaled naphthalene causes dose dependent Clara cell toxicity in mice but not in rats. *Tox Appl Pharmacol*. 2001; 173:114–119.
23. Plopper C, Chang A, Pang A, Buckpitt A. Use of microdissected airways to better define metabolism and cytotoxicity in murine bronchiolar epithelium. *Exp Lung Res*. 1991; 17:181–196. [PubMed: 2050024]
24. Kultz D, Li J, Gardell A, Sacchi R. Quantitative molecular phenotyping of gill remodeling in a cichlid fish responding to salinity stress. *Mol Cell Proteomics*. 2013; 12:3962–3975. [PubMed: 24065692]
25. Ranzinger R, Herget S, von der Lieth CW, Frank M. GlycomeDB--a unified database for carbohydrate structures. *Nucleic acids research*. 2011; 39:D373–D376. [PubMed: 21045056]
26. Morris JB. Nasal dosimetry of inspired naphthalene vapor in the male and female B6C3F1 mouse. *Toxicology*. 2013; 309C:66–72. [PubMed: 23619605]
27. Hanzlik RP, Koen YM, Theertham B, Dong Y, Fang J. The reactive metabolite target protein database (TPDB)--a web-accessible resource. *BMC. Bioinformatics*. 2007 Mar 16.8:95. 2007, 8, 95. [PubMed: 17367530]
28. Vila A, Tallman KA, Jacobs AT, Liebler DC, et al. Identification of protein targets of 4-hydroxynonenal using click chemistry for ex vivo biotinylation of azido and alkynyl derivatives. *Chem Res Toxicol*. 2008; 21:432–444. [PubMed: 18232660]
29. Jacobs AT, Marnett LJ. Systems analysis of protein modification and cellular responses induced by electrophile stress. *Accounts of chemical research*. 2010; 43:673–683. [PubMed: 20218676]

30. Burcham PC, Raso A, Kaminskas LM. Chaperone heat shock protein 90 mobilization and hydralazine cytoprotection against acrolein-induced carbonyl stress. *Mol Pharmacol.* 2012; 82:876–886. [PubMed: 22869587]
31. Tolson JK, Dix DJ, Voellmy RW, Roberts SM. Increased hepatotoxicity of acetaminophen in Hsp70i knockout mice. *Toxicol. Appl. Pharmacol.* 2006 Jan.210(1–2):157–162. *Epub.2005.Nov.8.* 2006, 210, 157–162. [PubMed: 16280147]
32. Hanzlik RP, Koen YM, Fang J. Bioinformatic Analysis of 302 Reactive Metabolite Target Proteins. Which Ones Are Important for Cell Death? *Toxicol Sci.* 2013
33. Li QK, Gabrielson E, Askin F, Chan DW, Zhang H. Glycoproteomics using fluid-based specimens in the discovery of lung cancer protein biomarkers: promise and challenge. *Proteomics Clin Appl.* 2013; 7:55–69. [PubMed: 23112109]
34. Sudhir PR, Chen CH, Pavana Kumari M, Wang MJ, et al. Label-free quantitative proteomics and N-glycoproteomics analysis of KRAS-activated human bronchial epithelial cells. *Molecular & cellular proteomics : MCP.* 2012; 11:901–915. [PubMed: 22761399]
35. Guo WA, Knight PR, Raghavendran K. The receptor for advanced glycation end products and acute lung injury/acute respiratory distress syndrome. *Intensive Care Med.* 2012; 38:1588–1598. [PubMed: 22777515]
36. Sukkar MB, Ullah MA, Gan WJ, Wark PA, et al. RAGE: a new frontier in chronic airways disease. *Br J Pharmacol.* 2012; 167:1161–1176. [PubMed: 22506507]
37. Lee CG, Da Silva CA, Dela Cruz CS, Ahangari F, et al. Role of chitin and chitinase/chitinase-like proteins in inflammation, tissue remodeling, and injury. *Annu Rev Physiol.* 2011; 73:479–501. [PubMed: 21054166]
38. Lee CG, Dela Cruz CS, Ma B, Ahangari F, et al. Chitinase-like proteins in lung injury, repair, and metastasis. *Proc Am Thorac Soc.* 2012; 9:57–61. [PubMed: 22550243]
39. Giannetti N, Moysé E, Ducray A, Bondier JR, et al. Accumulation of Ym1/2 protein in the mouse olfactory epithelium during regeneration and aging. *Neuroscience.* 2004; 123:907–917. [PubMed: 14751284]
40. Cai Y, Kumar RK, Zhou J, Foster PS, Webb DC. Ym1/2 promotes Th2 cytokine expression by inhibiting 12/15(S)-lipoxygenase: identification of a novel pathway for regulating allergic inflammation. *J Immunol.* 2009; 182:5393–5399. [PubMed: 19380786]
41. Hartl D, Lee CG, Da Silva CA, Chupp GL, Elias JA. Novel biomarkers in asthma: chemokines and chitinase-like proteins. *Curr Opin Allergy Clin Immunol.* 2009; 9:60–66. [PubMed: 19532094]
42. Sunil VR, Vayas KN, Massa CB, Gow AJ, et al. Ozone-induced injury and oxidative stress in bronchiolar epithelium are associated with altered pulmonary mechanics. *Toxicol Sci.* 2013; 133:309–319. [PubMed: 23492811]
43. Ge XN, Bahaie NS, Kang BN, Hosseinkhani MR, et al. Allergen-induced airway remodeling is impaired in galectin-3-deficient mice. *J Immunol.* 2010; 185:1205–1214. [PubMed: 20543100]
44. Trougakos IP. The molecular chaperone apolipoprotein J/clusterin as a sensor of oxidative stress: implications in therapeutic approaches - a mini-review. *Gerontology.* 2013; 59:514–523. [PubMed: 23689375]
45. Tripodi D, Quemener S, Renaudin K, Ferron C, et al. Gene expression profiling in sinonasal adenocarcinoma. *BMC medical genomics.* 2009; 2:65. [PubMed: 19903339]
46. Van Hal PT, Overbeek SE, Hoogsteden HC, Zijlstra FJ, et al. Eicosanoids and lipocortin-1 in BAL fluid in asthma: effects of smoking and inhaled glucocorticoids. *Journal of applied physiology (Bethesda Md. : 1985).* 1996; 81:548–555.
47. Ng FS, Wong KY, Guan SP, Mustafa FB, et al. Annexin-1-deficient mice exhibit spontaneous airway hyperresponsiveness and exacerbated allergen-specific antibody responses in a mouse model of asthma. *Clinical and experimental allergy : journal of the British Society for Allergy and Clinical Immunology.* 2011; 41:1793–1803. [PubMed: 22092555]
48. Pastor MD, Nogal A, Molina-Pinelo S, Melendez R, et al. Identification of proteomic signatures associated with lung cancer and COPD. *Journal of proteomics.* 2013; 89:227–237. [PubMed: 23665002]

49. Ray MK, Wang GY, Barrish J, Finegold MJ, Demayo FJ. Immunohistochemical localization of mouse clara cell 10-kd protein using antibodies raised against the recombinant protein. *J Histochem Cytochem.* 1996; 44:919–927. [PubMed: 8756763]
50. Buckpitt A, Chang AM, Weir A, Van Winkle L, et al. Relationship of cytochrome P450 activity to Clara cell cytotoxicity. IV. Metabolism of naphthalene and naphthalene oxide in microdissected airways from mice, rats, and hamsters. *Mol Pharmacol.* 1995; 47:74–81. [PubMed: 7838135]
51. Stripp BR, Maxson K, Mera R, Singh G. Plasticity of airway cell proliferation and gene expression after acute naphthalene injury. *Am J Physiol.* 1995; 269:L791–L799. [PubMed: 8572241]
52. Lakritz J, Chang A, Weir A, Nishio S, et al. Cellular and metabolic basis of Clara cell tolerance to multiple doses of cytochrome P450-activated cytotoxicants. I: Bronchiolar epithelial reorganization and expression of cytochrome P450 monooxygenases in mice exposed to multiple doses of naphthalene. *The Journal of pharmacology and experimental therapeutics.* 1996; 278:1408–1418. [PubMed: 8819528]
53. Lakritz J, Chang A, Weir A, Nishio S, et al. Cellular and metabolic basis of Clara cell tolerance to multiple doses of cytochrome P450-activated cytotoxicants. I: Bronchiolar epithelial reorganization and expression of cytochrome P450 monooxygenases in mice exposed to multiple doses of naphthalene. *The Journal of pharmacology and experimental therapeutics.* 1996; 278:1408–1418. [PubMed: 8819528]
54. Sies H. Role of metabolic H<sub>2</sub>O<sub>2</sub> generation: redox signaling and oxidative stress. *The Journal of biological chemistry.* 2014; 289:8735–8741. [PubMed: 24515117]
55. Winterbourn CC. The biological chemistry of hydrogen peroxide. *Methods Enzymol.* 2013; 528:3–25. [PubMed: 23849856]
56. Brigelius-Flohe R, Maiorino M. Glutathione peroxidases. *Biochimica et biophysica acta.* 2013; 1830:3289–3303. [PubMed: 23201771]
57. Barbour J, Neuhaus EM, Piechura H, Stoepel N, et al. New insight into stimulus- induced plasticity of the olfactory epithelium in *Mus musculus* by quantitative proteomics. *Journal of proteome research.* 2008; 7:1594–1605. [PubMed: 18336002]
58. Hanzlik RP, Koen YM, Fang J. Bioinformatic analysis of 302 reactive metabolite target proteins. Which ones are important for cell death? *Toxicol Sci.* 2013; 135:390–401. [PubMed: 23897987]
59. Lin CY, Isbell MA, Morin D, Boland BC, et al. Characterization of a structurally intact in situ lung model and comparison of naphthalene protein adducts generated in this model vs lung microsomes. *Chem Res Toxicol.* 2005; 18:802–813. [PubMed: 15892573]
60. Lame MW, Jones AD, Wilson DW, Segall HJ. Protein targets of 1,4-benzoquinone and 1,4-naphthoquinone in human bronchial epithelial cells. *Proteomics.* 2003; 3:479–495. [PubMed: 12687615]
61. Steentoft C, Vakhrushev SY, Joshi HJ, Kong Y, et al. Precision mapping of the human O-GalNAc glycoproteome through SimpleCell technology. *The EMBO journal.* 2013; 32:1478–1488. [PubMed: 23584533]

**Fig 1.**

Targeted quantitation of proteins with significant abundance changes in lung airway epithelium (LAE) and nasal olfactory epithelium (NOE) of mice exposed acutely or chronically to naphthalene. **A**) Extracted ion chromatograms of diagnostic peptides for secretoglobin from LAE of mice acutely exposed to naphthalene (blue) and controls (black). **B**) Ratios of EIC integrals for diagnostic secretoglobin peptides relative to the average in control mice (mean  $\pm$  SEM of 6 biological replicates). The overall average of all diagnostic peptides in naphthalene-exposed mice represents the AMT abundance ratio of secretoglobin in LAE (0.249). Note that the y axis in panel B is plotted on a log2 scale.

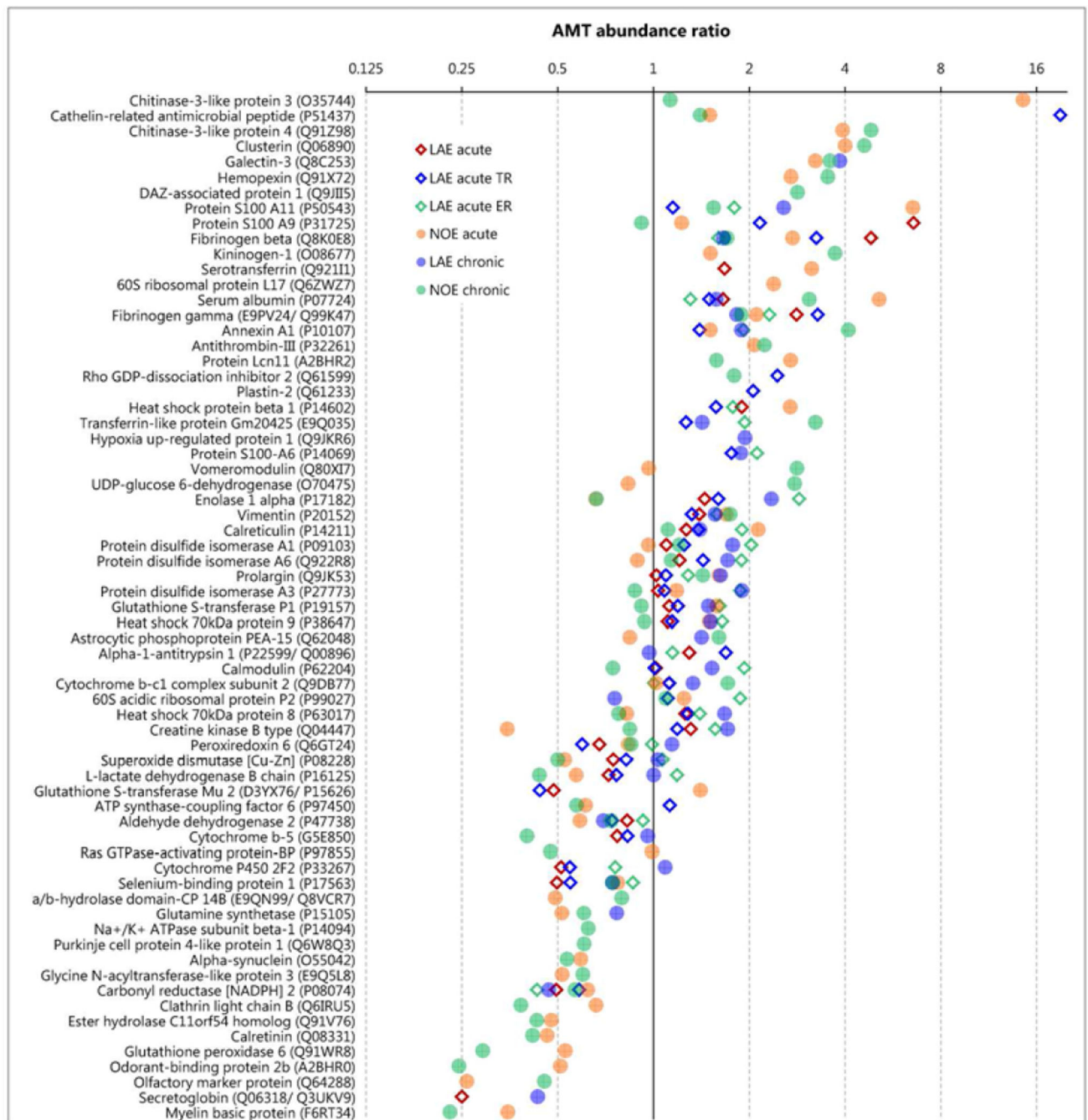


**Fig. 2.** AMT abundance ratio of proteins that are regulated in lung airway epithelium (LAE) and nasal olfactory epithelium (NOE) after acute (diamonds) and chronic (circles) naphthalene exposure of mice. Note that the y axis is plotted on a log<sub>2</sub> scale. LAE data on acute exposure of mice are accompanied by separate technical (TR) and experimental/ biological (ER) replicates.

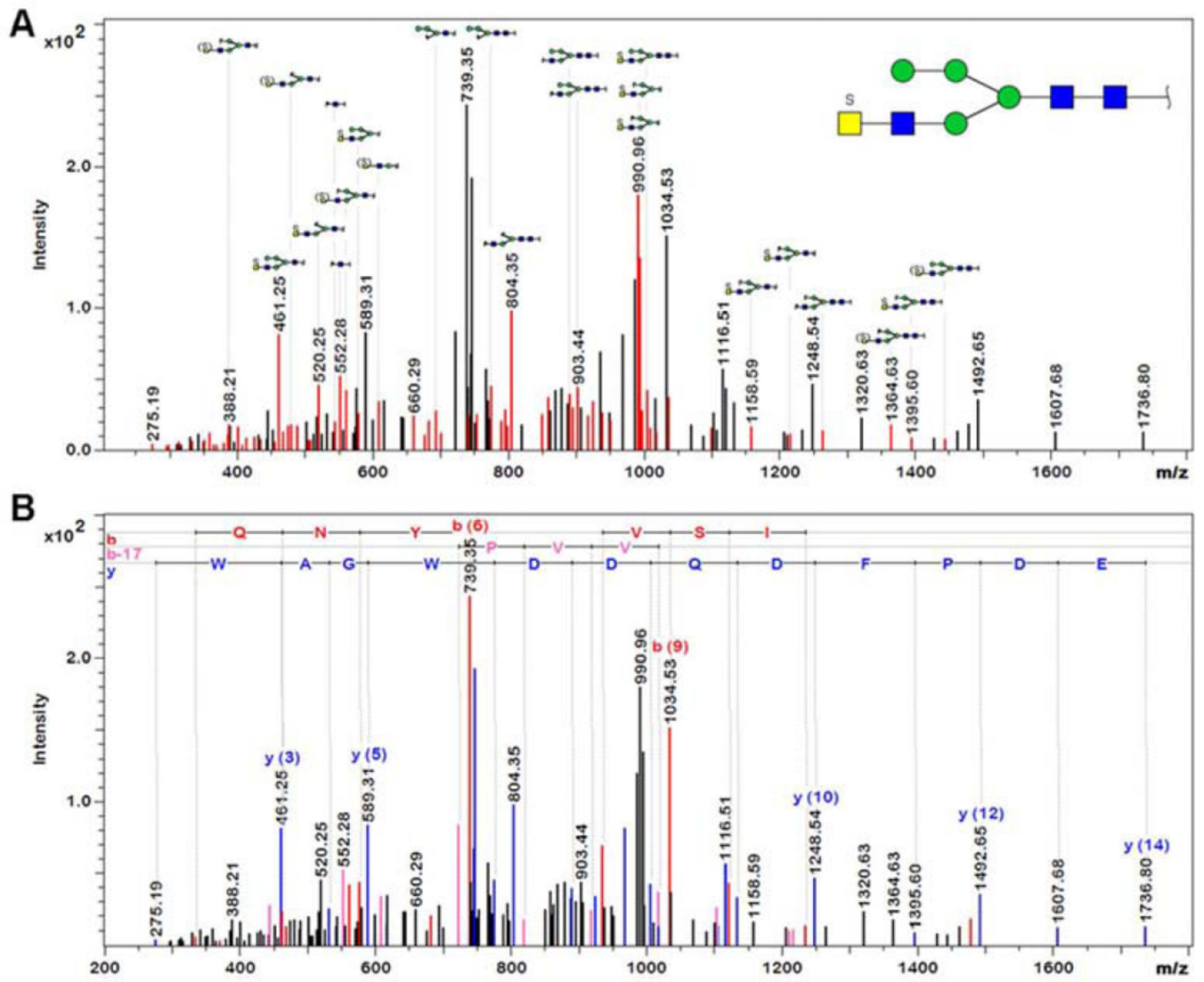


**Fig 3.**  
Identification of enolase 1 alpha (P17182) glycopeptide m/z 990.7895



**Table 1**

Abundance ratios for proteins targeted by reactive metabolites of lung toxicants

Protein	Quantitat. method	Abundance ratio (Naphthalene exposed/Control)				Notes on adduct formation			Protein function											
		Acute (n=6)/Control (n=6)	Acute (n=6) Control (n=6)	Nasal olfactory epithelium	Lung airway epithelium	Tolerant(n=6)/Control (n=6)	Species	Tissue		Chemical	Ref.									
(UniprotKB AC)		Lung airway epithelium (Technical replicates separated by colon)	Lung airway epithelium	Nasal olfactory epithelium	Lung airway epithelium	Nasal olfactory epithelium														
<b>Up regulated</b>																				
<b>Calreticulin (P14211)</b>	PA: 0.6, 0.7 SC: 3.2, 1.0 AMT: <b>1.3, 1.4</b>	1.0	1.0	1.2	1.3	1.0	1.0	1.2	1.3	1.0	Rat	Lung ( <i>in vivo</i> )	NN	[7]						Protein folding, Ca <sup>2+</sup> signaling
<b>Enolase 1 alpha non-neuron (P17182)</b>	PA: 1.2, 1.5 SC: 3.7, 0.7 AMT: <b>1.4, 1.6</b>	1.1	1.6	0.5	1.3	0.9	0.8	0.7	1.3	0.9	Mouse	Lung	BHT	[6]						Glycolysis
<b>Fibrinogen beta (Q8K0E8)</b>	PA: 2.5, 2.8 SC: 4.4, 2.2 AMT: <b>4.8, 3.3</b>	1.0	1.0	2.8	0.8	1.4	5.0	2.7	1.0	4.0	Monkey	Airway epithelium	NA	[10]						Platelet aggregation
<b>Glutathione S-transferase P1 (P19157)</b>	PA: 1.1, 0.9 SC: 0.8, 1.0 AMT: <b>1.1, 1.2</b>	1.4	1.5	1.2	1.2	0.9	1.4	1.6	1.5	1.2	Monkey	Airway epithelium	NA	[12]						Conjugation of electrophiles
<b>Heat shock protein beta 1 (P14602)</b>	PA: 1.5, 1.4 SC: 0.5 AMT: <b>2.81, 9, 1.6</b>	0.9	2.7	2.2	ND	ND	1.4	2.7	1.4	AMT: ND	Rat	Lung ( <i>in vivo</i> )	NN	[7]						Stress resistance, actin organization, chaperone
<b>Heat Shock 70 kDa protein 8 (P63017)</b>	PA: 1.1, 1.2 SC: 1.0, 1.1 AMT: <b>1.3, 1.3</b>	1.2	1.0	0.9	1.4	1.0	0.3	0.8	1.4	0.3	Mouse	Airways/ Lung	NA/BH T	[6, 59]						Repressor of transcriptional activation, chaperone
<b>Heat Shock 70 kDa protein 9 (P38647)</b>	PA: 1.0, 1.0 SC: 0.7, 2.2 AMT: <b>1.1, 1.1</b>	1.3	1.2	1.5	1.2	1.1	1.3	1.5	1.2	1.2	Rat/ Human	Nasal olfactory epithelium/ Bronchial epithelial cells	BQ/NQ	[60]						Protein folding, chaperone

Protein	Abundance ratio (Naphthalene exposed/Control)				Notes on adduct formation				Protein function	
	Acute (n=6)/Control (n=6)	Acute (n=6)/Control (n=6)	Tolerant(n=6)/Control (n=6)		Mouse/Rat/ Human	Airways/ Nasal olfactory epithelium/ Bronchial epithelial cells	NA/MC P			
<b>Protein disulfide isomerase A1</b> (P09103)	PA: 1.0, 1.1 (10/0), 1.4 SC: 1.1, 1.2/ AMT: 1.8	1.3 1.8 2.0	1.1 1.5 1.0	1.4 2.3 1.8	1.2 1.2 1.2				Rearrangement of disulfide bonds	
<b>Protein disulfide isomerase A3</b> (P27773)	PA: 1.0, 1.1 SC: 0.4, 1.6 AMT: 1.0, 1.1	1.1 0.5 1.9	0.8 1.5 1.2	1.1 (18/0) 1.9	1.1 2.0 0.9		NA/BQ /NQ	[9, 60]	Rearrangement of disulfide bonds	
<b>Vimentin</b> (P20152)	PA: 1.2, 1.3 SC: 0.9, 2.1 AMT: 1.4, 1.3	1.2 1.0 1.6	1.8 3.1 1.7	1.3 0.9 1.6	2.0 2.0 1.7		BHT	[6]		
<b>Fibrinogen gamma</b> (E9PV24/Q99K47/Q8VCM7)	PA: 2.1, 1.8 SC: (4/0), 9.0 AMT: 2.8, 3.3	0.9 (1/0) 2.3	1.5 (4/0) 2.1	0.7 ND 1.8	1.1 (5/0) 1.9				Platelet aggregation	
<b>Protein S100-A9</b> (P31725)	PA: 5.4, 2.4 SC: (9/0), AMT: (19/0) 6.6, 2.2	ND ND ND	1.6 (2/0) 1.2	ND (0/1) ND	1.1 2.0 0.9				Ca <sup>2+</sup> signaling	
<b>Protein S100-A11</b> (P50543)	PA: ND, 1.0 SC: (1/0), 3.0 AMT: ND, 1.2	1.1 3.2 1.8	1.9 (4/0) 6.5	1.2 1.9 2.6	2.4 1.5 1.5				Ca <sup>2+</sup> signaling	
<b>Annexin A1</b> (P10107)	PA: ND, 1.2 SC: (1/0), 1.9 AMT: ND, 1.4	1.5 1.6 1.9	1.3 (1/0) 1.5	1.2 1.2 1.9	1.8 (5/0) 4.1				Ca <sup>2+</sup> signaling	
Down regulated										
<b>Aldehyde dehydrogenase 2</b> (P47738)	PA: 0.7, 0.6 SC: 0.3, 0.7 AMT: 0.8, 0.7	0.7 0.3 0.9	1.1 0.3 0.6	0.6 0.5 0.7	0.8 (0/3) 0.7		NA	[8]	Aldehyde metabolism	
<b>ATP synthase, beta chain</b> (P56480)	PA: 0.9, 1.0 SC: 0.7, 1.7 AMT: 1.0, 1.1	1.1 1.0 1.1	1.2 0.6 1.2	0.9 0.7 1.6	0.7 0.9 0.8		NA	[8]	Oxidative phosphorylation chain	
<b>Bilirubin reductase</b> (Q923D2)	PA: ND, 1.3 SC: (0/2), 3.0 AMT: ND, 1.7	ND ND ND	0.8 0.2 0.9	ND ND ND	0.7 0.7 0.7		NN	[7]	Bilirubin synthesis	
<b>Creatine Kinase B type</b> (Q04447)	PA: 0.9, 1.0 SC: 0.2, 0.8 AMT: 1.3, 1.2	0.9 (0/5) 1.6	0.6 0.5 0.3	1.2 1.8 1.7	0.5 0.4 0.8		NA	[10]	Energy metabolism	

Protein	Abundance ratio (Naphthalene exposed/Control)			Notes on adduct formation			Protein function
	Acute (n=6)/Control (n=6)	Acute (n=6)/Control (n=6)	Tolerant(n=6)/Control (n=6)				
<b>Cytochrome b-c1 complex subunit 2</b> (Q9DB77)	PA: SC: AMT: 0.9, 1.2 0.5, 1.3 <b>1.4, 1.2</b>	0.9 1.6 <b>1.0</b>	ND ND <b>1.0</b>	1.0 1.0 <b>1.3</b>	1.2 (0/3) <b>1.7</b>	Rat  Nasal olfactory epithelium	NA [10] Oxidative phosphorylation chain
<b>Periredoxin 6</b> (O08709/Q6GT24)	PA: SC: AMT: 0.6, 0.7 0.1, 0.8 <b>0.8, 0.6</b>	0.8 0.4 <b>1.0</b>	0.9 2.8 <b>0.8</b>	0.9 0.8 <b>1.1</b>	1.0 1.9 <b>0.8</b>	Mouse Rat  Airway epithelium ( <i>in vivo</i> )	NA, NN, BHT [5, 7, 12] Cellular redox regulation
<b>Selenium binding protein 1</b> (P17563)	PA: SC: AMT: 0.5, 0.6 0.3, 0.3 <b>0.5, 0.5</b>	0.7 0.7 <b>0.9</b>	ND (1/0) <b>0.8</b>	0.7 0.3 <b>0.7</b>	0.7 1.2 <b>0.7</b>	Mouse Rat  Airway epithelium/ Lung ( <i>in vivo</i> )	NA, BHT NN [5, 7, 9] Sensing of reactive metabolites
<b>Superoxide dismutase [Cu-Zn]</b> (P08228)	PA: SC: AMT: 0.8, 0.7 0.3, 1.0 <b>0.7, 0.8</b>	1.0 0.3 <b>1.1</b>	0.7 1.4 <b>0.5</b>	1.2 1.8 <b>1.0</b>	0.6 1.1 <b>0.5</b>	Mouse  Lung	BHT [5] Metabolism of radicals to peroxide
<b>Vomeromodulin</b> (Q80XI7)	PA: SC: AMT: ND/ND ND/ND ND/ND	ND ND ND	ND S1.2 <b>1.0</b>	ND ND ND	2.02.0 <b>2.8</b>	Rat  Nasal olfactory epithelium	NA [10] Possible pheromone and odorant transporter
Not detected as adducted but are important proteins localized in the Clara cell							
<b>Cytochrome P450 2F2</b> (P33267)	PA: SC: AMT: 0.6, 0.7 0.1, (0/7) <b>0.5, 0.5</b>	ND (0/1) <b>0.5</b>	ND ND ND	0.7 ND <b>1.0</b>	ND ND ND		
<b>Secretoglobulin</b> (Q06318/Q3UKV9)	PA: SC: AMT: 0.3, ND 0.5, (0/4) <b>0.2, ND</b>	ND 0.3 ND	ND ND ND	0.3 0.2 <b>0.4</b>	ND ND ND		

ND = not detected, PA = Profile analysis 2.0 (Bruker Daltonics) ratio, SC = Spectral Count Scaffold 4.07) ratio, AMT: targeted accurate mass and time tag ratio, NA = naphthalene, NN = 1-nitronaphthalene, BHT = butylated hydroxyl toluene, MCP = monocrotalin pyrrole, NQ = 1,4- naphthoquinone, BHQ = benzoquinone. Acute 25-animals exposed for 4 hrs to 15 ppm naphthalene and tissues recovered 24 hrs after the completion of the exposure. Acute 31-animals exposed for 4 hrs to 15 ppm naphthalene and tissues recovered within 90 min of completion of the exposure. Tolerant 30-animals exposed daily to 15 ppm x 4 hrs naphthalene for 7 days and tissues were recovered 24 hrs after completion of the 7<sup>th</sup> day of exposure.

Table 2

Glycosylated peptides of naphthalene-reactive proteins. The glycosylation site is shown in bold and underlined. If multiple Asn, Ser, or Thr residues are present then the site with the highest NetNGlyc/NetOGlyc score [61] is indicated.

Protein name UniprotKB AC	Glycopeptide sequence	Range	Peptide Mr	Pep. m/z Glycopep.	m/z [ppm]	z	Peptide Scores (PS/MT/PX)	# Spectra		Glycome DB structure AC	Proteinscape Glycan structure	Glycan score	Glycan int. cov. (%)
								Lung	Nose				
<b>Calreticulin</b> P14211/ B2MWM9	K.GEWKPRQID NPDYK.G	273 – 286	1776.8113	<b>889.4129</b> 1218.5726	-17.90	2+	12.2/3.0	3		<b>4925</b>	Hex3Me2	26.9	23
<b>Enolase 1 alpha</b> P17182/ Q5FW97	K.KVN <del>V</del> VEQEK IDK.L	81 – 92	1427.7980	<b>714.9063</b> 1281.7475	-0.26	2+	21.3/D/5.3	2		<b>35086</b>		55.4	31
	K.SFVQNYPVVS IEDPFDQDDW GAWQK.F	282 – 306	2969.3468	<b>990.7895</b> 1427.6742	-1.35	3+	131.5/79.3/ 13.1	11		<b>10547</b>	Hex4HexNAc4S1	49.4	41
<b>Fibrinogen beta</b> Q3TCR2/ Q8K0E8	K.ENEN <del>V</del> INEYS SILEDQR.L	154 – 170	2050.9331	<b>1026.4784</b> 1564.7622	-1.02	2+	170.9/109.6/ 15.3	12	2	<b>9039</b>	HexNAc2S1	30.3	23
	K.YQVSV <del>N</del> K.Y	358 – 364	836.4355	<b>837.4428</b> 1235.6107	-4.42	1+	70.7/33.1/9.4	7		ND			
<b>Heat shock protein beta 1</b> P14602/Q545F4	K.AVTQSAEITIP VTEAR.A	176 – 192	1831.9528	916.9837 1274.6848	-8.29	2+	85.3/42.0/10.8	3		ND			
<b>Heat shock 70 kDa protein 8</b> P63017	R.RFDDAVVQS DMK.H	77 – 88	1409.6558	<b>705.8352</b> 1206.5931	-3.63	2+	131.1/88.3/ 10.7	11		<b>11077</b>		54.7	30
	K.LYOSAGGMP GGMPGGFPGG GAP <del>P</del> SGGASSG PTIEVD	610 – 646	3345.4978	<b>1116.1732</b> 1437.6768	1.78	3+	38.6/21.4/4.3	4		ND			
<b>Protein disulfide isomerase A1</b> P09103	R.TGPAAITLSD TAAAESLVDSSSE VTVIGFFK.D	135 – 164	2984.4897	<b>995.8372</b> 1228.6061	1.02	3+	126.2/77.8/ 12.1	7		<b>5383</b>	Hex10Me5	51.3	44
	K.VDAT <del>E</del> ESDLA QQYVVR.G	84 – 99	1779.8279	<b>890.9212</b> 1303.5879	0.22	2+	179.1/119.5/ 14.9	8		<b>5838</b>		14.8	13
	K.EECPAVRLITL EEEMTK.Y	312 – 328	2046.9839	<b>1024.4992</b> 1291.6275	-6.21	2+	11.5/2.9	1		<b>8090</b>		34.8	26
<b>Protein disulfide isomerase A3</b> P27773	R.DGKALEQFLQ EYFDG <del>N</del> LKR.Y	345 – 363	2270.1015	<b>1136.0540</b> 1206.6267	-17.47	2+	13.6/ND/3.4	11		<b>14035</b>	Hex1HexNAc3NeuAc1	23.3	15

Protein name UniprotKB AC	Glycopeptide sequence	Range	Peptide Mr	Pep. m/z Glycopep.	m/z [ppm]	z	Peptide Scores (PS/MT/PX)	# Spectra		Glycome DB structure AC	Proteinscape Glycan structure	Glycan score	Glycan int. cov. (%)
								Lung	Nose				
Vimentin P20152/ Q5FWJ3	K.VELQELNDRF ANYIDKVR.F	105 – 122	2221.1421	741.3880 1212.5536	-3.14	3+	66.8/36.4/7.6	1	ND				
	K.SRLGDLYEIE MREL.R	144 – 158	1910.9195	956.4670 1218.6135	2.01	2+	10.1/2.5	1	28495			33.7	19
	R.EEAESTLQSF RODVDNASLA R.L	197 – 217	2365.1117	789.3778 1241.5791	-1.23	3+	134.3/87.3/ 11.7	13	24797	Hex3HexNAc3Me2		26.4	12
	R.KVESLQEEIAF L.K.K	223 – 235	1532.8383	767.4264 1305.6783	-4.44	2+	131.5/85.6/ 11.5	12	26428	NAc2dHex1		49.7	25
	K.VESLQEEIAFL K.K	224 – 235	1404.7461	703.3803 1279.6444	-2.83	2+	80.6/53.7/6.7	14	ND				
	R.EEMENFALEA ANYQDTIGR.L	346 – 364	2199.9709	1100.9927 1332.6731	-1.55	2+	168.1/113.1/ 13.7	12	9297	Hex1NeuAc2S1		21.8	17
	R.LQDEIQNMK EEMAR.H	365 – 378	1733.8005	867.9075 1231.5778	-4.11	2+	146.7/90.6/ 14.0	13	9257	Hex1HexNAc1Me1S1		50.2	50
Aldehyde dehydrogenase 2 P47738	R.TFVQENVYD EFVER.S	327 – 340	1773.8230	887.9188 1206.5732	1.14	2+	134.8/92.4/ 10.6	9	25725			26.7	12
	R.AAFQLGSPW R.R	87 – 96	1147.5658	1148.5731 1395.6594	-10.12	1+	10.8/2.7	1	ND				
ATP synthase, beta chain P56480	R.IMDPNIIVGNE HYDVAR.G	407 – 422	1841.8671	921.9408 1464.7003	-3.22	2+	170.1/112.1/ 14.5	13	18039	Ac1NeuAc1		41.6	45
	K.SMAASGNLG HTPFLDEL.-	437 – 453	1758.8173	880.4159 1237.5837	-4.18	2+	125.6/74.4/ 12.8	11	ND				
Cytochrome b- c1 complex, subunit 2 Q9DB77	M.ATKCTKCGP GYSTPLEAMK. G	2 – 20	2098.9897	1050.5070 1232.5954	6.89	2+	13.2/3.3	5	3783	Hex4HexNAc1Me1		27.5	19
	R.NTGTEAPDYL ATVDVDPK.S	35 – 52	1904.8932	953.4579 1385.6875	0.50	2+	137.1/94.6/ 11.7	23	ND				
Superoxide dismutase [Cu- Zn] P08228	K.GDGPVQGTI HFEQK.A	11 – 24	1511.7379	756.8762 1365.6674		2+	99.1/55.8/10.8	25	ND				

Protein name UniprotKB AC	Glycopeptide sequence	Range	Peptide Mr	Pep. m/z Glycopep.	m/z [ppm]	z	Peptide Scores (PS/MT/PX)	# Spectra		Glycome DB structure AC	Proteinscape Glycan structure	Glycan score	Glycan int. cov. (%)
								Lung	Nose				
<b>Fibrinogen gamma</b> (E9PV24/ Q99K47/ Q8VCM7)	KGLIDEANQDF TNRINK.L	73 – 88	1846.9173	924.4604 1302.6199	-5.98	2+	44.4/16.5/7.0	2		22630	Hex3Me1	29.7	38
	RNIMEYLR.G	109 – 115	937.4691	938.4722 1231.6087	-4.52	1+	54.1/29.6/6.1	7	ND				
<b>Cytochrome P450 2F2</b> (P33267)	R.GDFANANNF DNITYGQVSEDL R.R	116 – 136	2346.0149	1174.0122 1263.5052	-2.14	2+	191.8/131.2/ 15.2	5		24491	Hex3HexNAc2dHex1	37.1	38
	R.EINLQDYEGH QK.Q	192 – 203	1472.6896	737.3537 1326.6282	2.22	2+	101.9/56.1/ 11.4	12	ND				
<b>Protein S100- A11</b> (P50543)	R.TSMPYTD <sup>u</sup> AVI HEVQR.F	344 – 358	1745.8449	873.9297 1249.6313	2.41	2+	117.2/78.8/9.6	9		36588		35.9	18
	K.YSGKDG <sup>u</sup> NNT QLSK.T	19 – 31	1410.6739	706.3394 1248.6109	-6.83	2+	84.3/44.7/9.9	6	ND				

ND = not determined